Photovoltaic and photo-capacitance effects in ferroelectric BiFeO$_3$ thin film

Pranab Parimal Biswas, Thirmal Chinthakuntla, Dhayanithi Duraisamy, Giridharan Nambi Venkatesan, Subramanian Venkatachalam, and Pattukkannu Murugavel

Photovoltaic and photo-capacitance effects in ferroelectric BiFeO$_3$ thin film

Pranab Parimal Biswas,[1] Thirmal Chinthakuntla,[1] Dhayanithi Duraisamy,[2]
Giridharan Nambi Venkatesan,[2] Subramanian Venkatachalam,[1]
and Pattukkannu Murugavel[1,a)]

[1]*Department of Physics, Indian Institute of Technology Madras, Chennai 600036, India*
[2]*Department of Physics, National Institute of Technology (NIT), Tiruchirappalli 620015, India*

A polycrystalline BiFeO$_3$ film on Pt/Ti/SiO$_2$/Si was fabricated using the spin coating technique. The film shows diode-like characteristics with and without poling measured under dark conditions. However, it exhibits a switchable photovoltaic effect with light illumination under poled conditions. The measured photovoltaic effect revealed an open circuit voltage of ~0.47 V and a short circuit current of 3.82 μA/cm^2 under the illumination of 165 mW/cm^2 irradiance. The studies clarified the dominant role of the depolarization field rather than the interface in the photovoltaic characteristics of the BiFeO$_3$ film. Significantly, the photo-capacitance effect was demonstrated with a substantial enhancement in capacitance (~45%) in Au/BiFeO$_3$/Pt geometry, which could open up a new window for BiFeO$_3$ applications. *Published by AIP Publishing.*
[http://dx.doi.org/10.1063/1.4983378]

Exploration of materials with additional degrees of freedom resulted in the growth of spintronics, magnetoelectrics, etc., with tremendous application potential.[1,2] Among them, the multiferroic BiFeO$_3$ (BFO) attracted renewed interest after the revelation of large polarization in an epitaxially grown film.[3] Large switchable polarization achieved by substrate induced strain,[1] doping,[4–6] and buffer layer[7] makes it an appealing candidate for ferroelectric random access memory (FeRAM) devices. High quality BFO films ensure their applications in ferroelectric tunnel junctions by manipulating the polarization direction dependent tunneling barrier width.[8]

Apart from these applications, the low bandgap (2.7 eV) of BFO unveiled a new dimension to its application potential towards photovoltaics (PV).[9–11] Switchable and tunable photovoltaic effects as a function of light intensity and wavelength, thickness, temperature, and doping have been explored in BFO films.[12–14] Various models are devised to explain the unconventional PV effect in ferroelectric materials in general. The bulk photovoltaic effect model shows that the asymmetric momentum distributions of photogenerated carriers are responsible for photocurrent in noncentrosymmetric ferroelectric crystals.[15] Very recently, an alternative explanation has been given using *ab initio* calculations, which suggests that the built-in potential step at the domain wall can give rise to an effective electric field of ~50 kV/cm^{-1}.[16] Interestingly, the switchable photocurrent is reported to be strongly affected by the electrode interface.[17] For example, Schottky junctions and depolarization fields are considered to influence the photovoltaic output in ferroelectric films.[18,19] However, there are reports revealing that the photocurrent in some BFO films cannot be switched and it is correlated with the formation of the depletion layer at the interface by oxygen vacancies.[20–22] Recently, an interesting polarization dependent simultaneous switching of diode

polarity and photovoltaic response is reported in epitaxial BFO films[20] and single crystals.[23] However, the PV studies are carried out mostly on either epitaxial or single crystalline samples. To understand the origin of the interface related PV response, we have carried out the PV studies on polycrystalline BFO films because of their preference towards application. The present study reveals the dominant role of the depolarization field rather than the interface in the PV characteristics of the BFO film. Remarkably, we observed the photo-capacitance effect on the fabricated film with as large as ~45% enhancement in capacitance under light illumination. The results presented in this letter will give an additional dimension to the application potential of BFO in fields such as ferroelectric random access memory (FeRAM) and spintronics.

The polycrystalline BFO film was deposited on the Pt(111)/Ti/SiO$_2$/Si(100) substrate by the spin coating technique using the reported procedure.[24] The film was characterized for its phase, morphology, and roughness using an X-ray diffractometer (Rigaku-Smart lab), an F50 field emission scanning electron microscope (FESEM), and an atomic force microscope (AFM) (Asylum), respectively. Its optical properties were probed using a UV-Visible spectrometer (JASCO-V-570). Semi-transparent Au dots of 200 μm diameter were used as top electrodes, and the resultant Au/BFO/Pt geometry was poled with $\pm$7 V. Positive and negative poling was done by applying respective positive and negative voltages to the bottom electrode. Photovoltaic measurements were carried out using a Keithley high resistance electrometer (6517B) with a Xenon arc lamp. A NumetriQ (PSM1375) phase sensitive multimeter was employed for capacitance and ac conductivity measurements. The polarization measurements were carried out using a Radiant Technology instrument (P-PMF).

The X-ray diffraction pattern as shown in Fig. 1(a) reveals the formation of the polycrystalline BFO film without any impurity phase which is a prerequisite for better
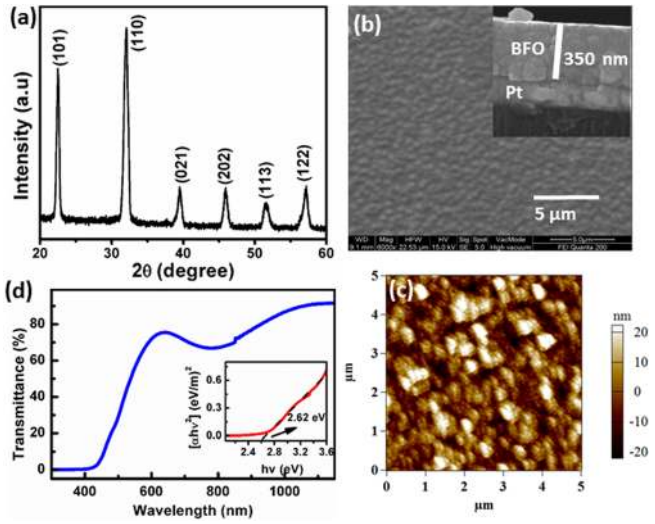
a)Electronic mail: muruga@iitm.ac.in

FIG. 1. (a) XRD pattern of the BFO film. (b) SEM image showing the surface morphology of the film; the inset shows its cross-sectional image. (c) AFM topographic image of the film. (d) Optical transmittance spectrum; the inset shows its Tauc's plot.
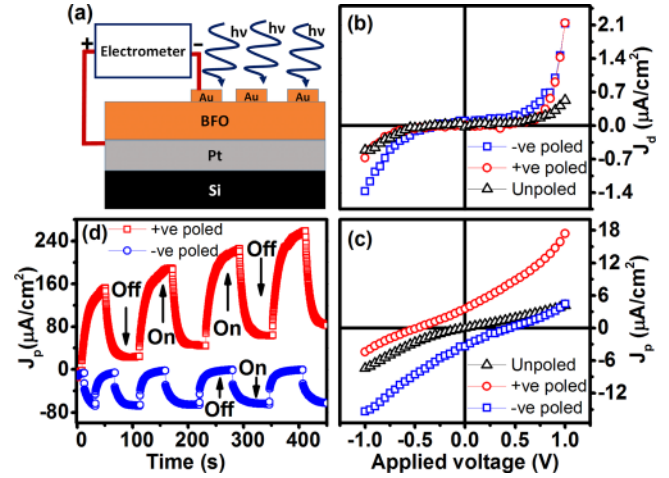

FIG. 2. (a) Schematic showing the geometry used for photovoltaic measurements. (b) J_d-V characteristics of BFO measured under dark. (c) J_p-V curves measured under light illumination. (d) ON-OFF curve for positive and negative poled states.

electrical properties. The film is crystallized in a rhombohedral structure. The FESEM image shown in Fig. 1(b) indicates the smooth surface without pin-holes, which would otherwise hamper the electrical measurements. The thickness and average roughness of the grown film are around 350 nm and 9 nm as indicated by the cross-sectional SEM image in the inset of Fig. 1(b) and the AFM topographic image shown in Fig. 1(c), respectively. The optical bandgap of the BFO film (deposited on the glass substrate) is estimated from the UV-Visible spectra shown in Fig. 1(d). The estimated bandgap from Tauc's plot [see the inset of Fig. 1(d)] is about 2.62 eV. The polarization (P) measured as a function of the electric field (E) on the Au/BFO/Pt capacitor (shown in Fig. S1, supplementary material) reveals the maximum remnant polarization ($2P_r$) value of 28 $\mu C/cm^2$. However, the large relaxation gap seen in the negative field region may come from charge defects (like oxygen vacancies) formed at the bottom interface.[21]

For photovoltaic measurements, Au/BFO/Pt capacitor geometry with light on top of the Au electrode is used as shown by the schematic in Fig. 2(a).The optical transmittance measurements performed on gold deposited on glass substrates show 32% transparency near the visible region (shown in Fig. S3, supplementary material), which is good enough for the PV effect. The dark current density (J_d) versus applied dc voltage (V) plotted without and with poling is shown in Fig. 2(b). The J_d-V curves represent a typical diode-like behavior with a threshold voltage of around 0.45 V. The BFO with a bandgap of 2.62 eV acts as a semiconductor, and the observed diode-like characteristics could come from the metal-semiconductor Schottky effect. Unlike the epitaxial BFO film,[20] we did not see any one-side diode effect in our as-grown BFO capacitor. This could be due to the difference in the growth process and metallic electrodes. The measurements are repeated under light illumination with 165 mW/cm^2 irradiance, and the results are shown in Fig. 2(c). Interestingly, the resultant photocurrent density (J_p)-V curves reveal the absence of diode-like characteristics.

It is observed that the cell shows photovoltaic effects with the resultant short circuit current density (J_{sc}) and open circuit voltage (V_{oc}) only for poled samples. The film shows J_{sc} values of 3.54 $\mu A/cm^2$ and $-3.22 \mu A/cm^2$ for positive and negative poling, respectively. The values are an order of magnitude higher than the values reported for the epitaxial BFO film.[20] The corresponding V_{oc} values are -0.47 V and 0.44 V. The switchable J_{sc} and V_{oc} confirm the dominant role of the polarization induced electric field in the photovoltaic effect. Note that the observed switchable PV effect is obtained without any need for special treatment like electrical training or thermal annealing usually adopted in the epitaxial film.

Further, the ON-OFF property under periodic exposure of light at ± 1 V shown in Fig. 2(d) reiterates the switchable photovoltaic effect. Photocurrent shows a rapid increase followed by slowly increasing current in the ON-state. Similarly, in the OFF-state, the photocurrent decreases rapidly and then slowly reaches its initial value. The possible reason for the ON/OFF slow increase/decrease in current could be the heating/cooling effect of BFO causing the change in the resistance of the sample.[25] However, the role of the pyroelectric effect cannot be completely discarded in the observed photocurrent. To verify it, simultaneous photocurrent and temperature measurements are carried out on the sample under continuous illumination as a function of time. The resultant current plot shows a step-like function when the light is ON and thereafter remains constant with time (shown in Fig. S4, supplementary material). On the other hand, the temperature plot reveals an initial rapid increase followed by a gradual change with time. Since the pyroelectric current is proportional to $\frac{dP}{dT}$, where P is the polarization and T is the temperature, the current is expected to largely decrease with time as per the observed increase in temperature. Incidentally, the current is almost constant with time ruling out the possibility of major current contribution coming from the pyroelectric effect.

To explain the PV effect, energy-band diagrams for the Au/BFO/Pt structure are drawn using the reported work functions (φ) of 5.1, 5.3, and 5.6 eV of Au, Pt, and BFO,

respectively, and the electron affinity (χ) of 3.3 eV of BFO. The resultant band diagrams are shown in Fig. 3. Although there are reports for BFO being n-type,[26] we assumed it to be a p-type semiconductor[21,22] largely because of oxygen vacancies. The difference in work functions suggests that the metal-semiconductor contacts are indeed Schottky junctions. The depletion region at the junctions can be modulated by oxygen vacancies and polarization switching. Typical diode-like characteristics of the J-V curves observed for unpoled BFO in the dark can be understood from the wide width of the Schottky barrier shown in Fig. 3(a). However, electron-hole (e-h) pair generations under illumination turn the Schottky barriers into Ohmic contacts [see Fig. 3(b)]. Note that under the unpoled condition, the BFO did not show the PV effect [see Fig. 2(c)] due to the lack of the depolarization field and hence resulted in Ohmic-like J-V curves. On the other hand, when the device is positively poled (+P state), there could be a reduction in the barrier at the bottom interface [as shown in Fig. 3(c)] by the migration of oxygen vacancies into bulk due to poling.[27] It may be noted that the as-prepared BFO sample was reported to have accumulation of oxygen vacancies at the bottom interface.[23] In the same way, the barrier width could increase when the device is negatively poled as shown in Fig. 3(e). However, under illumination, the barriers turn into Ohmic [as shown in Figs. 3(d) and 3(f)] and the generated e-h pairs in bulk get separated by the depolarization field with the resultant photovoltaic effect as seen in Fig. 2(c).

To investigate the capacitance response to polarization directions and light illumination, we have carried out the capacitance measurements on the BFO capacitor. The capacitance under dark and illumination for unpoled and poled states measured from 1 kHz to 1 MHz is shown in Fig. 4(a). The capacitance exhibits a substantial increment under poling and shows a further enhancement after illumination. The frequency dependence of the percentage change in capacitance ($\%\Delta C = \frac{C_p - C_{up}}{C_{up}} \times 100$, where C_p and C_{up} are the capacitance measured after poling under dark/light and before poling under dark, respectively) is plotted in Fig. 4(b). The capacitance shows a remarkable change of nearly 32% at 1 kHz for the poled state with an additional 13% upon shining light for the unpoled state under dark conditions. The effect can be attributed to the increase in charge
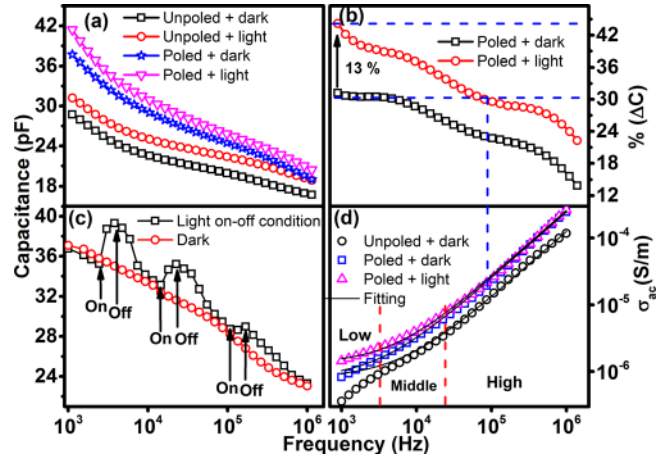
FIG. 4. (a) Capacitance as a function of frequency before and after poling with and without illumination. (b) $\%\Delta C$ versus frequency plot for the poled state under dark and illumination with respect to the unpoled state under dark. (c) The capacitance versus frequency plot under light ON-OFF and dark conditions. (d) Frequency dependent ac-conductivity measured with and without light on the unpoled and poled sample.

contribution due to the alignment of dipoles and e-h pair generation for the former and latter case, respectively. The photo-capacitance effect is again reiterated from the ON-OFF measurement on the poled sample shown in Fig. 4(c). The observed photo-capacitance can have a direct impact on FeRAM applications where the information can be written electrically and read optically.

To investigate it further, the corresponding frequency dependent ac-conductivity is plotted in Fig. 4(d). The plots indicate three regions viz., low frequency regions due to the electrode polarization effect masking the bulk ionic conduction, middle regions due to dc-conductivity contribution, and high frequency regions due to bound charges associated with the dipoles in the sample.[27] Fig. 4(d) shows that at frequencies above 100 kHz, the frequency-dependent conductivity is unaffected by the light illumination ruling out the contribution from the e-h pair (which do not respond at high frequency anyway) and the heavy ions, which would otherwise increase the conductivity.[28] Further, the conductivity follows Jonscher's power law $\sigma_{ac} = \sigma_{dc} + A\omega^n$,[27] where σ_{dc} is the dc-conductivity, ω is the frequency, A is a pre-exponential constant, and n is a fitting parameter ($0 < n < 1$). The extracted values of σ_{dc} for unpoled, poled, and poled under light states are 7.1×10^{-7}, 7.9×10^{-7}, and 13.0×10^{-7} S/m, respectively. The dc-conductivity is slightly increased from the unpoled to poled state, which is expected as the number of free charge carriers contributing to the dc-conductivity is the same. But the change is significant under illumination due to electron-hole pair generation.

It is interesting to see that the decrease in $\%\Delta C$ from low frequency to 100 kHz under illumination, beyond which the e-h pairs will not respond, is the same ($\sim$13%) as the initial increment in $\%\Delta C$ upon shining light in the poled state at 1 kHz [marked in Fig. 4(b)]. This confirms the dominant role of e-h pair generated carriers in the photo-capacitance effect seen at low frequencies. Since the heavy ion contribution is ruled out at high frequency from our conductivity measurements, the continued enhancement in capacitance observed beyond 100 kHz may originate from light-induced
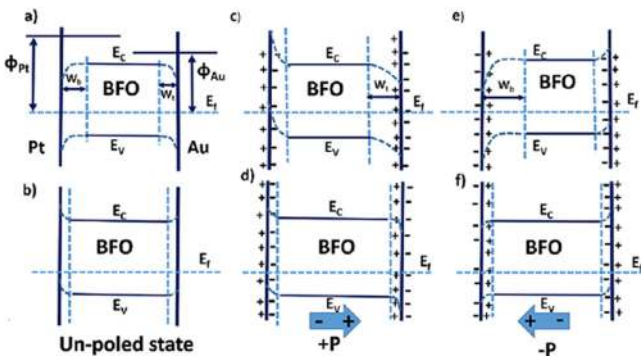

FIG. 3. Schematic energy band diagrams illustrating the variation in Schottky barriers for BFO under (a) dark and (b) illumination in unpoled, (c) dark and (d) illumination in positively poled, and (e) dark and (f) illumination in negatively poled states.

dipoles in the sample. Note that such light induced dipole related polarization is reported in several materials.[29,30] Overall, the studies bring out the dominant role of e-h pair generated carriers in the observed photo-capacitance effect.

In conclusion, the fabricated $Au/BiFeO_3/Pt/TiO_2/SiO_2/Si$ sample exhibited Schottky diode-like characteristics without and with poling conditions measured under dark. It is noteworthy to mention that the sample under study showed photovoltaic effects only under poled conditions, which concludes that the interface plays a limited role in the observed photovoltaic effect in the polycrystalline BFO sample unlike the epitaxial film where the interface played an important role. The switchable photovoltaic effect was demonstrated in the polycrystalline $BiFeO_3$ film with the maximum observed V_{oc} of 0.47 V. Importantly, the photo-capacitance effect was demonstrated in the $Au/BiFeO_3/Pt$ sample under poled and illumination conditions with 32% and an additional 13% change in capacitance, respectively. This effect is further illustrated in the capacitance study carried out in the light ON-OFF state. Overall, the photo-capacitance demonstrated in the $BiFeO_3$ film can be envisaged in applications related to FeRAM (writing electrically and reading optically), ferroelectric tunnel junctions, and other optoelectronics applications.

See supplementary materials for further details about the polarization versus electric field hysteresis loop, J-V curve, and photocurrent and temperature measured as a function of time under continuous light illumination of the BFO film along with the transmission spectra of the gold film deposited on the glass substrate.

[1]D. Sando, A. Agbelele, D. Rahmedov, J. Liu, P. Rovillain, C. Toulouse, I. C. Infante, A. P. Pyatakov, S. Fusil, E. Jacquet, C. Carrétéro, C. Deranlot, S. Lisenkov, D. Wang, J.-M. Le Breton, M. Cazayous, A. Sacuto, J. Juraszek, A. K. Zvezdin, L. Bellaiche, B. Dkhil, A. Barthélémy, and M. Bibes, Nat. Mater. **12**, 641 (2013).

[2]M. Bibes and A. Barthélémy, Nat. Mater. **7**, 425 (2008).

[3]J. Li, J. Wang, M. Wuttig, R. Ramesh, and N. Wang, Appl. Phys. Lett. **84**, 5261 (2004).

[4]S. K. Singh, H. Ishiwara, and K. Maruyama, Appl. Phys. Lett. **88**, 262908 (2006).

[5]S. K. Singh, H. Ishiwara, K. Sato, and K. Maruyama, J. Appl. Phys. **102**, 094109 (2007).

[6]K. Abe, N. Sakai, J. Takahashi, H. Itoh, N. Adachi, and T. Ota, Jpn. J. Appl. Phys. **49**, 09MB01 (2010).

[7]J. Wu, S. Qiao, C. Pu, D. Xiao, J. Wang, and J. Zhu, Appl. Phys. A **109**, 57 (2012).

[8]V. Garcia, S. Fusil, K. Bouzehouane, S. Enouz-Vedrenne, N. D. Mathur, A. Barthelemy, and M. Bibes, Nat. Lett. **460**, 81 (2009).

[9]R. Palai, R. S. Katiyar, H. Schmid, P. Tissot, S. J. Clark, J. Robertson, S. A. T. Redfern, G. Catalan, and J. F. Scott, Phys. Rev. B **77**, 014110 (2008).

[10]T. P. Gujar, V. R. Shinde, and C. D. Lokhande, Mater. Chem. Phys. **103**, 142 (2007).

[11]C. M. Hung, C. S. Tu, W. D. Yen, L. S. Jou, M. D. Jiang, and V. H. Schmidt, J. Appl. Phys. **111**, 07D912 (2012).

[12]J. Seidel, D. Fu, S. Y. Yang, E. Alarcón-Lladó, J. Wu, R. Ramesh, and J. W. Ager III, Phys. Rev. Lett. **107**, 126805 (2011).

[13]S. Y. Yang, L. W. Martin, S. J. Byrnes, T. E. Conry, S. R. Basu, D. Paran, L. Reichertz, J. Ihlefeld, C. Adamo, A. Melville, Y. H. Chu, C. H. Yang, J. L. Musfeldt, D. G. Schlom, J. W. Ager III, and R. Ramesh, Appl. Phys. Lett. **95**, 062909 (2009).

[14]R. K. Katiyar, Y. Sharma, D. Barrionuevo, S. Kooriyattil, S. P. Pavunny, J. S. Young, G. Morell, B. R. Weiner, R. S. Katiyar, and J. F. Scott, Appl. Phys. Lett. **106**, 082903 (2015).

[15]V. Fridkin, Crystallogr. Rep. **46**, 654 (2001).

[16]S. Y. Yang, J. Seidel, S. J. Byrnes, P. Shafer, C.-H. Yang, M. D. Rossell, P. Yu, Y.-H. Chu, J. F. Scott, J. W. Ager III, L. W. Martin, and R. Ramesh, Nat. Nanotechnol. **5**, 143 (2010).

[17]M. Qin, K. Yao, and Y. C. Liang, Appl. Phys. Lett. **95**, 022912 (2009).

[18]J. Zhang, X. Su, M. Shen, Z. Dai, L. Zhang, X. He, W. Cheng, M. Cao, and G. Zou, Sci. Rep. **3**, 2109 (2013).

[19]M. Qin, K. Yaoand, and Y. C. Liang, Appl. Phys. Lett. **93**, 122904 (2008).

[20]D. Lee, S. H. Baek, T. H. Kim, J. G. Yoon, C. M. Folkman, C. B. Eom, and T. W. Noh, Phys. Rev. B. **84**, 125305 (2011).

[21]H. Matsuo, Y. Kitanaka, R. Inoue, Y. Noguchi, and M. Miyayama, Appl. Phys. Lett. **108**, 032901 (2016).

[22]H. Matsuo, Y. Kitanaka, R. Inoue, Y. Noguchi, and M. Miyayama, J. Appl. Phys. **118**, 114101 (2015).

[23]T. Choi, S. Lee, Y. J. Choi, V. Kiryukhin, and S. W. Cheong, Science **324**, 63 (2009).

[24]A. Srivastava, A. Garg, and F. D. Morrison, J. Appl. Phys. **105**, 054103 (2009).

[25]V. S. Puli, D. K. Pradhan, R. K. Katiyar, I. Coondoo, N. Panwar, P. Misra, D. B. Chrisey, J. F. Scott, and R. S. Katiyar, J. Phys. D: Appl. Phys. **47**, 075502 (2014).

[26]R. Nechache, C. Harnagea, S. Li, L. Cardenas, W. Huang, J. Chakrabartty, and F. Rosei, Nat. Photonics **9**, 61 (2015).

[27]A. K. Jonscher, Nature **267**, 673 (1977).

[28]R. K. Katiyar, A. Kumar, G. Morell, J. F. Scott, and R. S. Katiyar, Appl. Phys. Lett. **99**, 092906 (2011).

[29]F. R. Marcos, A. D. Campo, P. Marchet, and J. F. Fernańdez, Nat. Commun. **6**, 6594 (2015).

[30]H. S. Kim, S. K. Kim, B. J. Kim, K. S. Shin, M. K. Gupta, H. S. Jung, S. W. Kim, and N. G. Park, J. Phys. Chem. Lett. **6**, 1729 (2015).